THE HEAT AND FLUID FLOW ANALYSIS FOR WATER HEATER

by

Chien-Nan LIN [a*]***, Cheng-Chi WANG*** [a]***, and Yi-Pin KUO*** [b]

[a] Department of Mechanical Engineering, Far East University, Hsin-Shih, Tainan, Taiwan
[b] Department of Electronic Engineering, Far East University, Hsin-Shih, Tainan, Taiwan

Original scientific paper
UDC:66.046:662.75:519.254
DOI: 10.2298/TSCI11S1081L

In this paper, the heat transfer and fluid flow are studied for the water heater of RV cars, in which the hot water is heated by the combustion energy of liquefied petroleum gases. Three types of combustion tubes are performed in this investigation, which are circular tube, elliptic tube and elliptic tube with screwed wire inserted. The heat transfer performances of numerical simulation results are compared with those of the experimental works; they are in good trend agreement. The elliptic combustion tube performs better than the circular one, which indicates the average 7% energy saving for the elliptic combustion tube and 12% energy saving for the elliptic combustion tube with screwed wire under static heating.

Key words: *numerical simulation, water heater, combustion*

Introduction

Water heaters are widely used in various industrial and domestic applications for hot water. The heating energy may come from different kinds of resources, such as petroleum fuel, natural gas, electrical power or solar energy. And combustion is still the convenient way to produce thermal energy for outdoor uses. The recreation vehicle is one example, in which the water heater adopts liquefied petroleum gases or liquefied natural gas as fuel. The combustion reaction occurs in the combustion chamber, which is enclosed by the water tank filling with cold water. The thermal energy is then transferred from the produced gases through the chamber walls to the cold water within the tank. The structure of the water heater is shown in fig. 1. The fuel is injected from a nozzle and flows through a Ventura tube to induce the first inlet fresh air. The mixed gases are led to the combustion chamber through the gas tube, and the second inlet air is also supplemented near the outlet of the mixed gas tube to make up the proper air to fuel ratio.

It is difficult to measure the temperatures and gases flow distributions in the combustion chamber by experimental work due to the high temperatures, which are normally above 2000 K. Therefore, the numerous numerical simulations were widely used to analyze the heat and fluid flow in these years [1-4]. Saade and Kozinski's research [5] presented and

* Corresponding author; e-mail: lincn@cc.feu.edu.tw

validated in a series of combustion of fibrous sludge experiments. Roux *et al*. [6] studied the numerical simulations in a premixed swirled combustor, and used the LES model combined with acoustic analysis; the numerical results quite matched the experimental data.

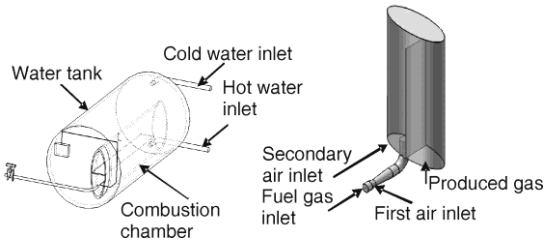

Figure 1. The construction of water heater

Considering the energy consumptions saving, Yutaka *et al*. [7] used the honeycomb regenerator to exchange the heat between the exhausted gas and the preheated air and fuel to increase the heat efficient; the temperature of the preheated air was up to 1600 K, and they also reduced the NO_x production in their experiment. Zhang and Nieh [8] studied a novel vortex combustor, which is characterized by a strong swirl and low temperature combustion environment. The results show that the swirl provides an effective control of the gas-particle slip velocity in the vortex combustor.

This study aims to increase the heat flux by improving the combustion chamber in the water heater. The heat flux is described by the equation of $Q = UA\Delta T$. The temperature difference, ΔT, is between the combusted produced gases and the cold water. The overall heat transfer coefficient, U, is determined by the heat convection coefficient at both sides of the combustion tube, which depends on the heat transfer coefficients and the thermal conductivity of the combustion tube. The heat transfer coefficient, *h*, and the contacted area, *A*, are further considered to enhance the heat transfer rate in this study. However, a screwed wire is inserted in the second combusted chamber to increase the gas mixture, which is a passive device to increase the heat transfer coefficient. Also, the larger contact area can be adopted by squeezing the combustion chamber from circular shape to be elliptic shape. Under the same volume of combustion chamber, the elliptic tube performs larger surface area to volume ratio (*A*/*V*) than circular tube.

Theory analysis

Three types of combustion tubes are analyzed in this investigation including circular tube, elliptic tube and elliptic tube with screwed wire inserted. The combustion tubes are separated into two chambers by a baffle plate, which enlarges the length of the flow channels to increase the wall heat flux between the gases and cold water. The geometric diagrams of the three combustion tubes are shown in fig. 2. The combustion tube is placed inside the water tank to heat the cold water. Considering the water tank capacity, the volume of the elliptic tube (πabL) is equal to the volume of the circular tube ($\pi r^2 L$). The diameter of the combustion tube is 4 inches for the circular pipe, and the elliptic tubes are made of five-inch circular pipes, and squeezed to be 1:2:7 of aspect ratio.

The continuity equation, momentum equation, energy equation and species diffusive equations are as follows:

$$\frac{\partial}{\partial x_i}(\rho u_i) = 0 \tag{1}$$

$$\frac{\partial}{\partial x_i}(\rho u_i u_j) = -\frac{\partial p}{\partial x_i} + \frac{\partial}{\partial x_i}\left[\mu\left(\frac{\partial u_i}{\partial x_j} + \frac{\partial u_j}{\partial x_i} - \frac{2}{3}\delta_{ij}\frac{\partial u_l}{\partial x_l}\right)\right] + \frac{\partial}{\partial x_j}(-\rho\overline{u_i' u_j'}) \tag{2}$$

$$\nabla \cdot [\vec{\upsilon}(\rho E + p)] = \nabla \cdot \left[k_{\text{eff}} \nabla T - \sum_j h_j \overrightarrow{j_j} + (\tau)(\bar{\bar{\tau}}_{\text{eff}} \vec{\upsilon}) \right] + S_{\text{h}} \tag{3}$$

$$\nabla(\rho \vec{\upsilon} Y_i) = -\nabla \vec{J}_i + R_i \tag{4}$$

where $\overline{u_i' u_j'}$ is Reynolds stress, $\overline{u_j' T'}$ is Reynolds heat flux, E is total internal energy, Y_i is mass fraction of species O_2 ,N_2 and C_3H_8, J_i is diffusion flux, R_i is mass source term due to combustion reaction.

Propane gas was used as the fuel in this combustion mode, and the finite rate volume reaction combustion is considered in this study. The chemical reaction equation is:

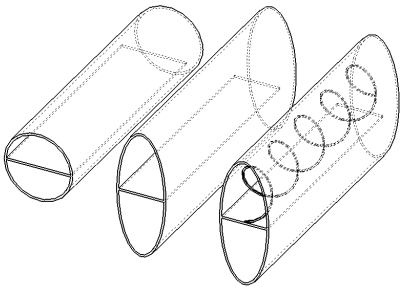

Figure 2. (a) the circular combustion tube (b) the elliptic combustion tube (c) the elliptic combustion tube inserted screw wire

$$C_3H_8 + 5(O_2 + 3.76N_2) \rightarrow 3CO_2 + 4H_2O + 18.8N_2 + \Delta Q \tag{5}$$

The standard two equation κ–ε model was adopted in the simulation; they are:

$$\frac{\partial}{\partial x_i}(\rho u_i \kappa) = \frac{\partial}{\partial x_i}\left[\left(\mu + \frac{\mu_{\text{t}}}{\sigma_{\text{k}}}\right)\right] + G_{\text{k}} + G_{\text{b}} - \rho\varepsilon \tag{6}$$

$$\frac{\partial}{\partial x_i}(\rho u_i \varepsilon) = \frac{\partial}{\partial x_i}\left[\left(\mu + \frac{\mu_{\text{t}}}{\sigma_{\varepsilon}}\right)\frac{\partial \varepsilon}{\partial x_j}\right] + c_1 \frac{\varepsilon}{k}(G_{\text{k}} + c_3 G_{\text{b}}) - c_2 \rho \frac{\varepsilon^2}{k} \tag{7}$$

where G_{k} is the production of turbulence kinetic energy, G_{b} – the generation of turbulence

The fuel inlet pressure was set as 1500-5000 Pa in gauge pressure and the temperature is set to be 300 K. The inlet and outlet pressure are considered as pressure boundary condition of atmosphere and the temperature is set to be 300 K.The conjugated heat transfer occurs in the chamber wall, and the heat conduction equation is solved. The exterior wall of combustion chamber is set to be the temperature of water.

Numerical scheme

The CFD Fluent 6.2 code is applied to analyze the combustion heat transfer. Grid independence is tested for different combustion chamber; the errors are controlled within 0.5 K of average temperature differences exhausted gas at outlet boundary. The SIMPLE scheme is used to solve the pressure-velocity coupling equations; first order upwind scheme is used to treat the convective terms. The total grids of combustion chamber are 600,000 after the grids test for three sets of grids numbers; they are about 400,000, 600,000 and 800,000. The errors of wall heat flux are less than 1% between 600,000 and 800,000, and the estimated numerical error is 2.6% by numerical convergence analysis in this numerical simulation.

Experimental analysis

The outline of experimental configure is shown in fig. 1; the liquefied petroleum gas were supplied from the storage tank, where the flow rate is throttled by the regulator, and the

ignition are controlled by the electric sparker to produce the initial combustion. The mass flow meter is used to measure the flow rates of the petroleum gases; the accuracy is within 0.1% of measured range. The accuracy of the pressure transmitter is 1% of span range. The variable area type is adopted in the flow meter for the dynamic test, and the accuracy is controlled within 2%. The K-type thermocouples are placed at the inlet and outlet tube of air and water sides. The total experimental uncertainty is 4% for the static heating and 5% for the flooding heating in this measurement.

Results and discussions

The temperature distributions and contours at different sections location are shown in fig. 3. The mixture of fuel gas and air are injected into the left chamber side, and then combusted reaction occurs at the ignited region. The produced gases flow through the head region along the right side chamber and are exhausted to the outside. fig. 3(a) displays that the temperature increases rapidly and then gradually decays along the gases flowing paths due to heat transfer to the chamber wall. By comparing the temperature profiles of the three cases, it is found that the average temperatures at different section planes of the circular type are higher than those of the other two types, which shows that the heat flux is the lowest in the circular type. Also, the elliptic chamber with screwed wire inserted demonstrates lower temperature profiles than the types without wire inserted. The temperature distributions at the second chamber are uniform at every section plane for case 1. Contrarily, the temperatures adjacent to the cold water are higher than those of baffle side for elliptic chamber, which is due to the flowing of most gas along the wall of cold water side.

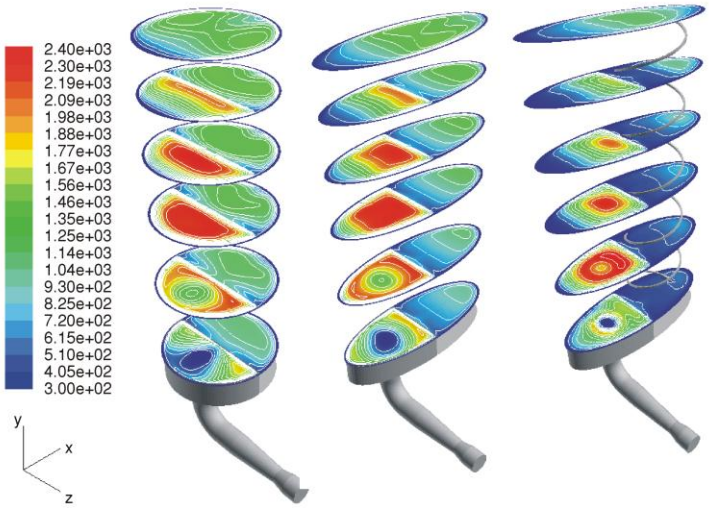

Figure 3. The temperature contours at different y-plane section; (a) circular combustion tube, (b) elliptic combustion tube; (c) elliptic combustion tube inserted screw wire

The streamlines released from the fuel inlet and velocity distributions are displayed as fig. 4. The gases flow straightly to the chamber head and change the direction through the secondary chamber to the outlet. Circulating flow appears at the secondary chamber of case 3;

the produced gas flows around the screwed wire and the flow path is longer than others, which enhances the perturbation of exhausted gas and increases the heat transfer rate. The mixture of fuel and air leaves the outlet of the mixed tube, which causes the maximum velocity to appear. And then the mixture flows into the enlarged chamber, inducing the secondary air into the chamber. The maximum velocity slightly decays and appears in the central regions of the first chamber due to the boundary layer effect. When the produced gases flow around the top of the combustion chambers, the maximum velocities appear along the water side wall and flow faster than the neighbor fluid near the baffle plane due to the inertial forces.

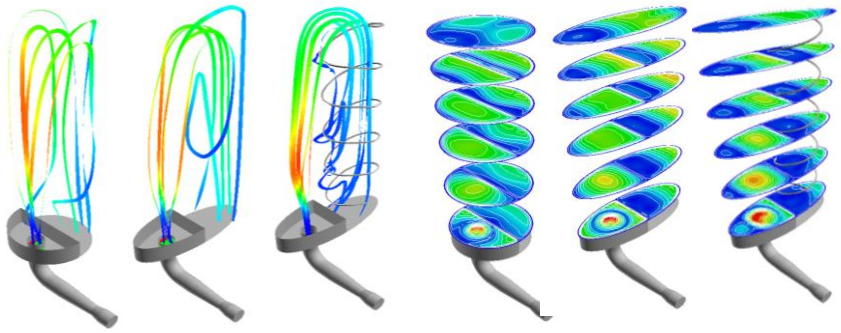

Figure 4. The streamlines and velocities contours for the three combustion chambers

The diagram of the heat flux in the combustion tube walls varied with tank water temperature for the three types of chambers are shown in fig 5. The heat transfer rate decreases with the temperature of the surrounding cold water due to the lower temperature difference between produced gases and the cold water. And the heat flux of the circular combustion tube is averagely 7% lower than that of the elliptic tube without screw wire, and 12% lower than that of the elliptic tube with inserted screw wire. The outlet temperatures of the exhausted gas at the exit of the combustion chamber also are shown in fig. 5. This reveals that the gas outlet temperature will increase with the water temperature for both the experimental and numerical results. While the cold water receives thermal energy to increase the temperature, it will cause that the temperature differences between these two fluids decreases and the heat flux is reduced. The gas outlet temperature, therefore, increases to the degree as the temperature of the cold water. The experimental data are also shown in fig. 5; the temperatures are averagely about 30-45 °C higher than the numerical results, which yields 10-14% differences. The differences caused by the thermocouples receive the radiation heat from the produced gases inside the combustion chamber. If we compare case 3 with case 2, it is obvious that the temperature gradient field is steeper for case 3, this is because the inserted screwed wire disturbs the flow streams; more heat is transferred to the wall, inducing the lower exit temperature for case 3.

Conclusions

The investigation of the three types of combustion tubes circular tube, elliptic tube and elliptic tube with screwed wire are performed in this study.

- The elliptic combustion tubes perform better than the circular one. For example, the

elliptic combustion tubes with and without the screwed wire are able to save 12% and 7% of energy under static heating.

- The circulating flow appears at the secondary chamber of elliptic chamber with screwed wire inserted, which enhances the perturbation of exhausted gas and increases the heat transfer rate.
- The results of the numerical simulation are in considerably good agreement with the experimental work; the average deviations are about 10-14%.

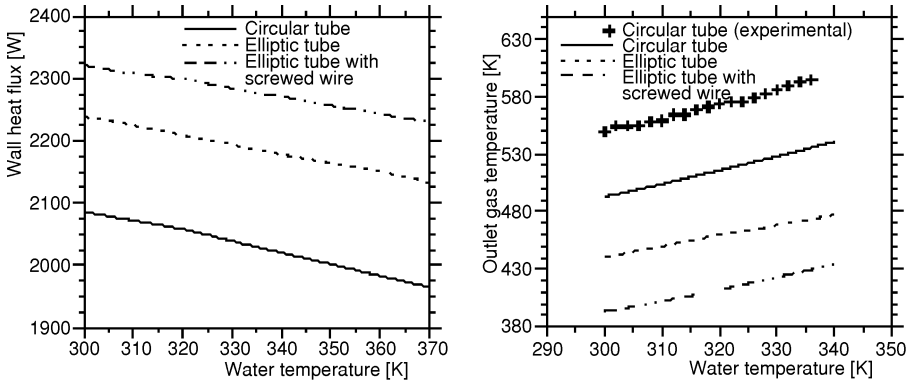

Figure 5. The wall heat flux and outlet gas temperature for different water temperatures

References

[1] Furuhata, T., *et al*., Performance of Numerical Spray Combustion Simulation, *Energy Conversion and Management, 38* (1997), 10-13, pp. 1111-1122

[2] Koh, P. T. L., Nguyen, T. V., Jorgensen, F. R. A., Numerical Modeling of Combustion in a Zinc Flash Smelter, *Applied Mathematical Modeling, 22* (1998), 11, pp. 941-948

[3] Mitsuru, Y., *et al*., Modeling of Eddy Characteristic Time in LES for Calculating Turbulent Diffusion Flame, *International Journal of Heat and Mass Transfer, 45* (2002), 11, pp. 2343-2349

[4] Yin, C., *et al*., Investigation of the Flow, Combustion, Heat-transfer and Emissions from a 609 MW Utility Tangentially Fired Pulverized-Coal Boiler, *Fuel, 81* (2002), 8, pp. 997-1006

[5] Raafat, G. S., Janusz, A. K., Numerical Modeling and TGA/FTIR/GCMS Investigation of Fibrous Residue Combustion, *Journal of Biomass & Bioenergy, 18* (2000), 5, pp. 391-404

[6] Roux, S., *et al*., Studies of Mean and Unsteady Flow in a Swirled Combustor Using Experiments, Acoustic Analysis, and Large Eddy Simulations, *Combustion and Flame, 141* (2005), 1-2, pp. 40-54

[7] Yutaka, S., *et al*., Heat Transfer Improvement and NO_x Reduction by Highly Preheated Air Combustion, *Energy Conversion and Management, 38* (1997), 10-13, pp.1061-1071

[8] Zhang, J., Nieh, S., Swirling, Reacting, Turbulent Gas-Particle Flow in a Vortex Combustor, *Powder Technology, 112* (2000), 1-2, pp.70-78

Paper submitted: July 12, 2010
Paper revised: September 16, 2010
Paper accepted: November 11, 2010